

Comprehensive Study of Cu-Doped ZnO Nanoparticles: Structural, Dielectric, and Optical Insights

M. Hansson, E. Lindström, K. Johansson*

*Department of Physics, Lund University, Lund, Sweden

ABSTRACT

The structural, morphological, optical and electrical studies of Cu doped Zinc Oxide (ZnO) nanoparticles which were synthesized by hydrothermal method. The PXRD results confirmed that the synthesized material is polycrystalline ZnO and the average crystallite size of the Cu doped ZnO were determined by using the Scherrer's formula. Various functional groups were analyzed by using the FTIR analysis. Surface morphological and chemical compositions were analyzed using SEM and EDX. The optical properties were carried out using transmission and Photoluminescence spectrum. The dielectric properties of the Cu doped ZnO nanoparticles dielectric constant, dielectric loss, AC conductivity were analyzed in various frequencies and temperatures at specific conditions.

Keywords: Cu-doped ZnO nanoparticles; hydrothermal; Optical and dielectric studies.

I. INTRODUCTION

Nanotechnology may be able to create many new materials and devices with a vast range of applications, such as in medicine, electronics, biomaterials and energy production. On the other hand, nanotechnology raises many of the same issues as any new technology, including concerns about the toxicity and environmental impact of nonmaterial's and their potential effects on global economics, as well as speculation about various scenarios. ZnO is a promising material for the realization and future of nanotechnology ZnO can be utilized for electronic and photonic devices, as well as for high-frequency applications. ZnO is transparent to visible light and can be made highly conductive by doping. ZnO has a long history of usage for pigments and protective coatings on metals. The electrical, optoelectronic and photochemical properties of undoped ZnO has resulted in use for solar cells, transparent electrode and blue/UV light emitting devices [1-5]. ZnO films have low electric resistance and high transparency in the visible range. Several deposition techniques have been used to grow ZnO thin films, including sol-gel process, spray pyrolysis, molecular beam epitaxy (MBE), chemical vapor deposition (CVD) and sputtering [6-11]. In comparison with other techniques, the solution route method has the advantage of being low cost and low substrate temperature deposition. In this paper, the preparation of Cu-doped ZnO nanoparticles and their structural, surface morphology, optical and dielectric studies have been reported.

II. EXPERIMENTAL PROCEDURE

All chemicals were purchased and used as received without further purification. Initially, (1M) Zinc acetate was mixed with 70 ml of deionized water and 30 ml of ethanol and the mixed solution was stirred and (0.01M) Cupric nitrate was mixed with 70 ml of deionized water and 30 ml of ethanol and mixed the solutions. Then ammonia solution was added drop wise into solution. The initial solution was blue in color. Finally, NaOH solution was added into it until the complete precipitation occurred. The container of the solution was placed in a water bath, and the temperature was kept at 60° for 2h. Filtered precipitates were dried in oven at 700°C constant temperature.

III. RESULTS AND DISCUSSION

Fig. 1 shows the powder XRD pattern of Cu doped ZnO nanoparticles. The diffraction patterns can be indexed to the hexagonal wurtzite phase. The crystal phase of the ZnO samples agreed with the standard data of wurtzite structure. The strongest diffraction peaks corresponding to (101), (002) and (100) plane reveals that the synthesized ZnO have samples are highly single crystalline nature. No peaks belonging to secondary phases Cu was detected, which is confirms the purity of the samples and dopant metal ions can substitute in the regular lattice site of ZnO. The average crystallite size of the Cu doped ZnO was found to be 12 nm.

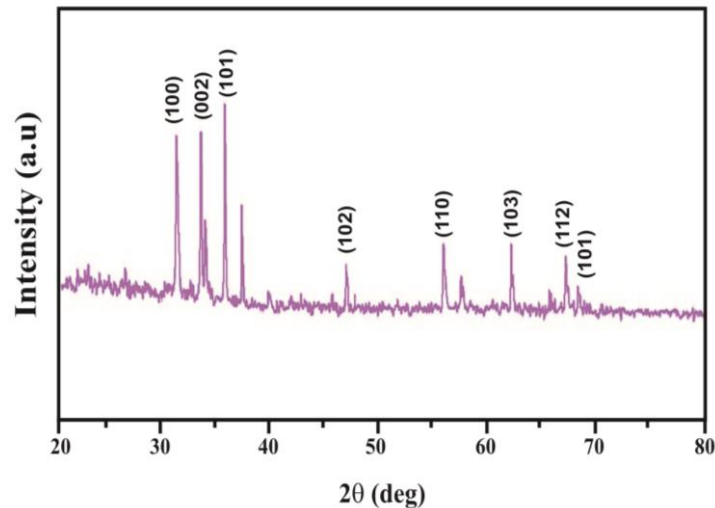


Fig.1. XRD pattern of Cu doped ZnO

FTIR is a technique used to obtain information about the chemical bonding in a material. It is used to identify the elemental constituents of a material. Fig.2 shows the FTIR spectrum of Cu doped ZnO s. In pure ZnO, the vibration bands appeared at 3428 and 1594 cm^{-1} , which is related to O–H stretching vibration and O–H–O bending vibration respectively [12]. The strong peak appeared at 454 cm^{-1} is related to stretching vibration of O–Zn. There is no absorption peak related to O–Cu, which is confirms the substitution of these metal ions in ZnO lattice.

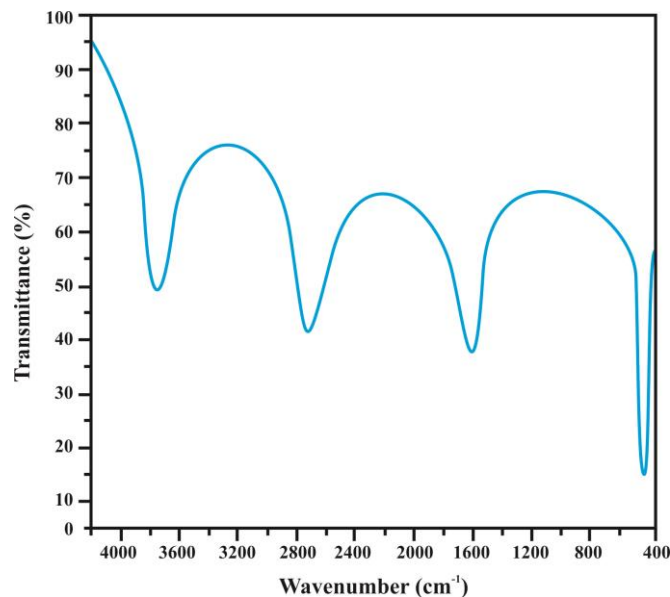


Fig.2 FTIR spectrum of Cu doped ZnO

Scanning electron microscopy (SEM) is one of the most widely used techniques for the characterization of size and morphology of the particles. The SEM images of the Cu-doped Zn nanoparticles are shown in Fig.3. It is clearly seen that the microstructure formed is found to be uniform and compact structure which are interconnected by grains. These results suggested that, the size of the grains is large. Fig.4 shows the results of the qualitative elemental analysis done by the energy dispersive X-ray analysis (EDX) for Cu-doped ZnO nanoparticles. The EDX spectrum exhibited clear peaks corresponding to Cu, Zn and O.

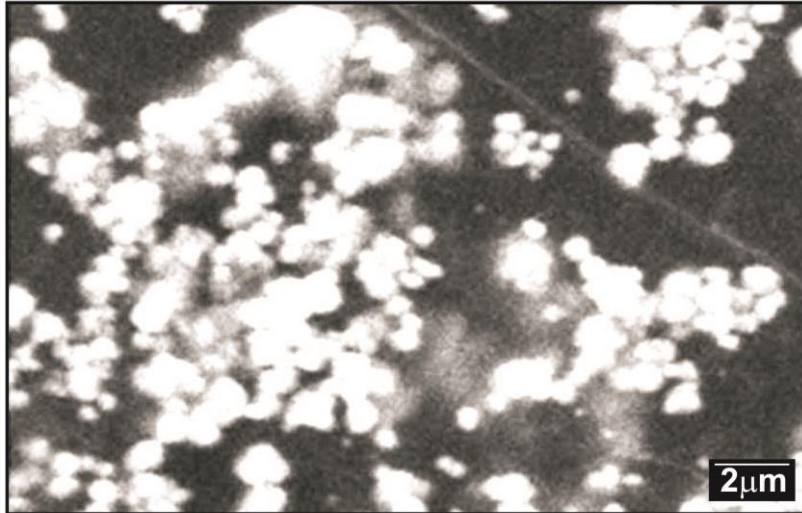


Fig.3. SEM Image of Cu doped ZnO

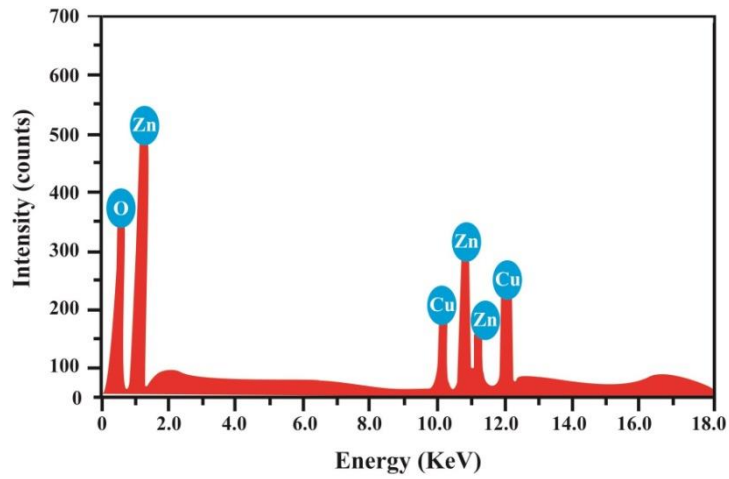


Fig.4. EDX spectrum of Cu doped ZnO

To study the influence of Cu doping on the photoluminescence of ZnO, the room temperature photoluminescence measurements were carried out (as shown in Fig. 5) at the excitation wavelength of 325 nm. A strong UV emission at 378 nm and along with several relatively weak visible emissions peaks were observed at 432 nm (blue emission) and 532 nm (green emission). Generally, the UV emission is attributed to free excitonic emission near band edge (NBE) [13]. The blue emission is related to transmission mediated defect such as band gap and oxygen vacancies and Zn interstitials. The green emission is peak is generally due to the oxygen vacancies, among them 532 nm is related to single oxygen (V_o^+) [14].

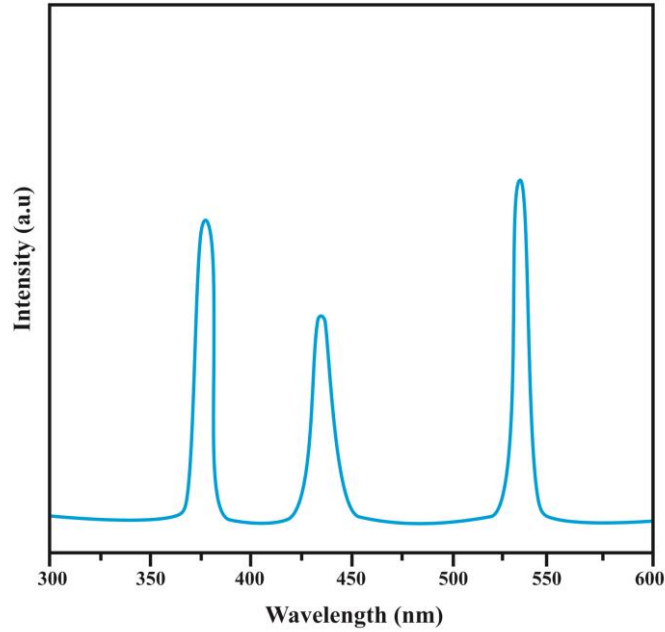


Fig.5 PL spectrum of Cu doped ZnO

UV–Vis transmission spectrum measurement was performed on the Cu doped ZnO in the UV–Vis region at room temperature as shown in Fig.6. The optical transmission of Cu doped ZnO was higher than the ZnO. Further, absorption edge was shifted to longer wavelength (red-shift) for Cu doped ZnO. This may be due to decreasing the band gap energy and also surface plasmon resonance effect. The band gap values were thus determined by the extrapolation of the linear portion of the $(\alpha h\nu)^2$ curve versus the photon energy $h\nu$. The band gap energy was found to be 2.90eV for Cu doped ZnO and enlightened by the p–d spin-exchange interactions between the band electrons and the localized d electrons of the transition-metal ion substituting the Cu^{2+} ion. In addition, the band gap drop due to doping of Cu concentration is mainly due to the strong p–d mixing of O and Cu [15].

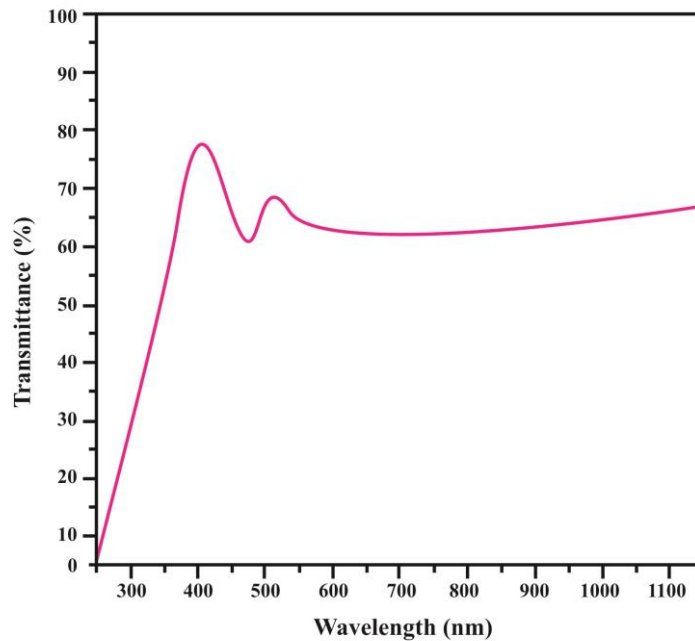


Fig.6 Transmission spectrum of cu doped ZnO

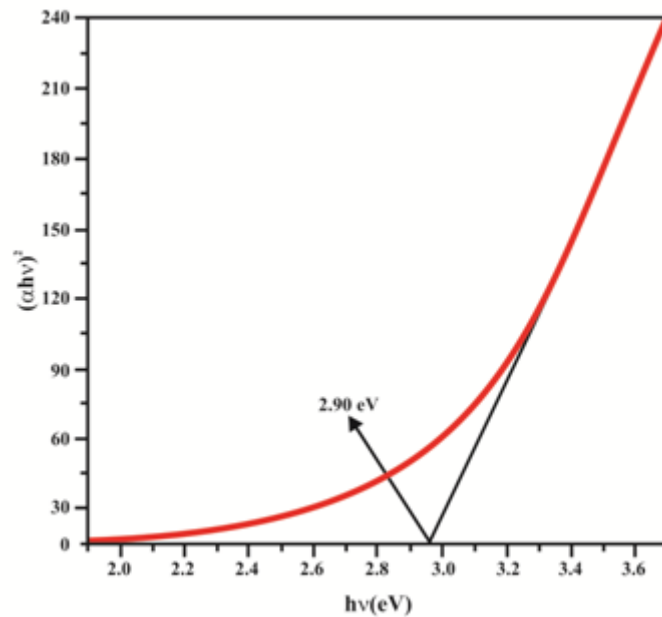


Fig.7 Optical bandgap of Cu doped ZnO

The Cu-doped ZnO nanoparticles pellets in disk form were studied at various temperatures. The variation of the dielectric constant with frequency and temperature for the Cu doped ZnO nanoparticles is shown in Fig.8. The dielectric constant of Cu doped ZnO nanoparticles is high at low frequencies that decrease rapidly in the applied frequency at all temperatures. The high value of the dielectric constant might be ascribed to the increased ion jump orientation effect and the increased space charge effect showed by the nanoparticles [16]. Most of the atoms in the nanocrystalline materials reside in the grain boundaries, which become electrically active as a result of charge catching. The dipole moment can easily follow the changes in the electric field, particularly at low frequencies. In this way, the dielectric constant of nanostructured materials should be larger than that of the conventional materials [7]. One reason for the large value of the dielectric constant of nanocrystalline materials at adequately high temperature is the increased space charge polarization because of the structure of their grain limit interfaces [18]. Likewise, at adequately high temperature the dielectric loss is ruled by the sharp increase of the dielectric constant at lower frequencies and at lower temperatures. As temperature increases, the space charge and ion jump polarization decreases, resulting in a decrease in the dielectric constant [19].

The variations of the dielectric loss of the Cu doped ZnO with frequency and temperature are shown in Fig.9. It can be seen that the dielectric loss decreases with the increase of frequency and at higher frequencies the loss angle has practically a similar value at all temperatures. The orientations of molecules along the direction of the applied electric field in polar dielectrics require a part of the electric energy to overcome the forces of internal friction [20]. A part of the electric energy is used for revolutions of dipolar molecules and different kinds of molecular transfer from one position then onto the next, involving energy losses. The AC conductivity plot of the palletized type of form of pure and Cu-doped ZnO nanoparticles is shown in Fig.10. There is a small increase in the electrical conductivity of the nanomaterial at the low frequency region for an increase in the frequency and is the same for all temperatures. It is seen that the frequency independent behavior at a lower frequency region, which characterizes the DC conductivity and the dispersion at higher frequency region shows the frequency dependent behavior. It is consistent with the increase in temperature resulting in an enormous carrier hopping that causes the increase in the conductivity [21].

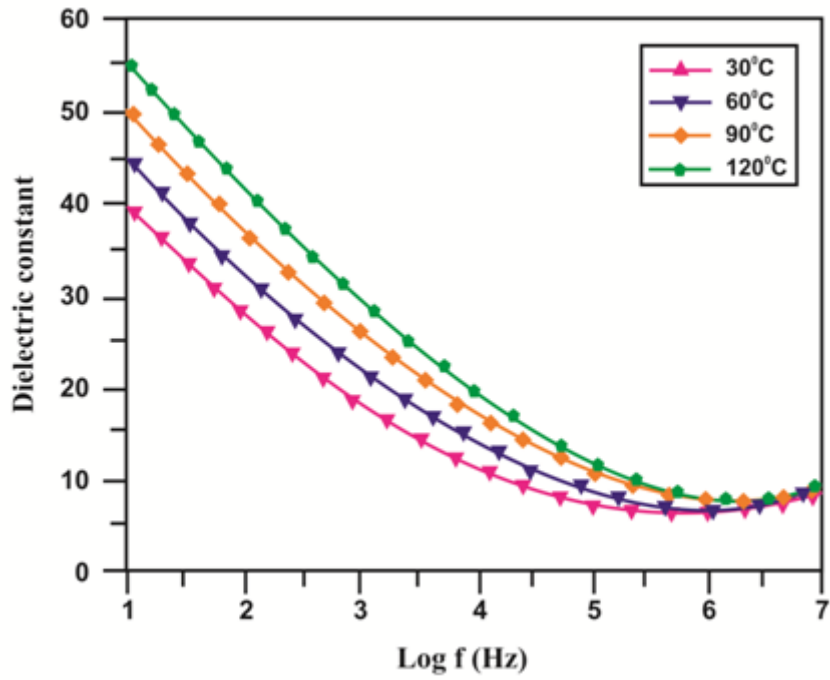


Fig.8 Variation of dielectric constant with frequency

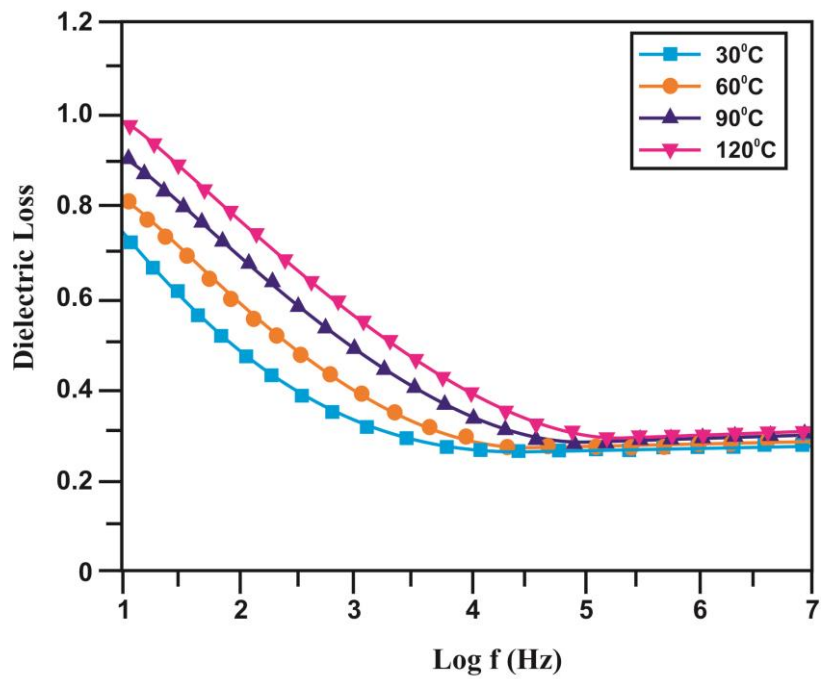


Fig.9 Variation of dielectric loss with frequency

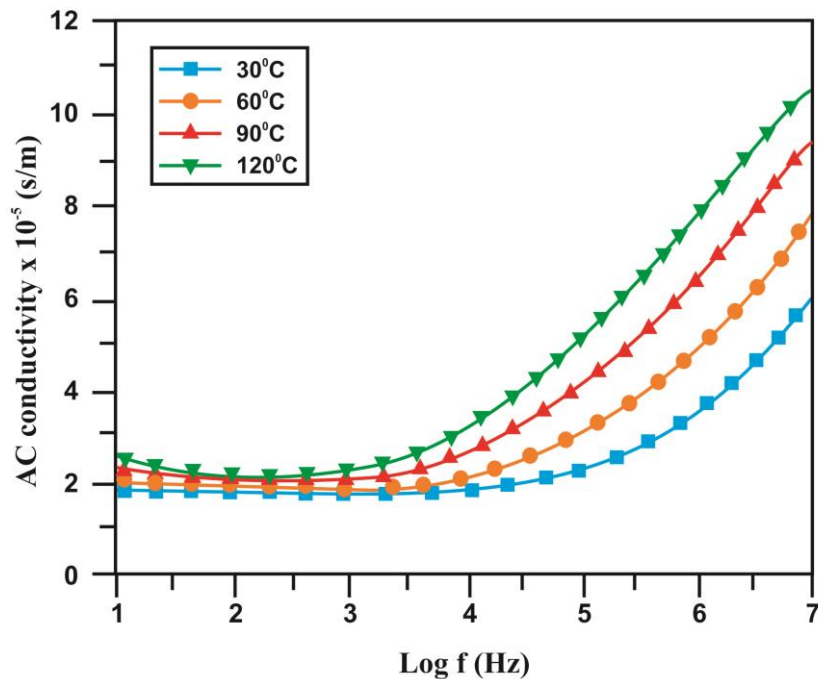


Fig.10 Variation of AC conductivity with frequency

IV. CONCLUSIONS

Cu-doped ZnO nanoparticles were prepared by the hydrothermal method. From the XRD analysis, it was identified that the obtained polycrystalline ZnO with hexagonal wurtzite structure and the average crystallite size of the Cu doped ZnO was found to be 12 nm. The different functional groups were confirmed by using FTIR analysis. The SEM observation clearly showed the fact that the particles were aggregated. UV-Vis spectrum revealed that the Cu doped ZnO particle absorption occurred in the UV region. The estimated band gap values for the Cu-doped ZnO nanoparticles were found to be 2.90 eV. The oxygen defect and reduction band gap energy of ZnO was another crucial role in enhancing photocatalytic performance of ZnO, which is confirmed through PL studies. The variations of the dielectric constant, the dielectric loss, and AC conductivity with frequency and temperature for the Cu doped ZnO nanoparticles were performed. The dielectric studies revealed that both the dielectric constant and the dielectric loss varied inversely, i.e., (decreased) with the frequency. The AC electrical conductivity was found to be directly proportional to the temperature and the frequency.

V. REFERENCES

1. D. G. Baik and S. M. Cho, *Thin Solid Films*, 354(1999), 227
2. Y. Ohya, M. Ueda And Y. Takahashi, *Jpn. J. Appl. Phys.*,35 (1996), 4738.
3. Y. Natsume, *Thin Solid Films*, 372(2000), 30.
4. G. K. Paul, S. Bandyapadhyay And S. K. Sen, *Phys. Status Solid A*,191(2002),509.
5. D.C. Look, D. C. Reynolds, C. W. Litton And G. Cantwell, *Appl. Phys. Lett.*, 81 (2002), 1830.
6. P Sagar , M Kumar., R.M. Mehra, *Thin Solid Films*, 489 (2005), 94.
7. Baik D.G, S.M Cho., *Thin Solid Films*, 354 (1999), 227.
8. P. Fons, K. Iwata, S. Niki, A. Yamada, K. Matsubara, *J. Cryst. Growth*, 209 (2000), 532.
9. K. Sakurai, D.Iwata, S. Fujita, S. Fujita, *Jpn. J. Appl. Phys.*,138 (1999), 2606.
10. Y.Liu, C.R.Gorla, S.Liang, N. Emanetoglu, Y.Lu, H. Shen, *J. Electron. Mater.*,29 (2000), 69.
11. J.L. Vossen, *Phys. Thin Films*, 9 (1977)1.
12. A.J. Reddy, M.K. Kokila, H. Nagabhushan, R.P.S. Chakradhar, C. Shivakumar, J.L. Rao, B.M. Nagabhushan, *J. Alloys Compd.* **509**, 5349–5355 (2011)
13. P. Sagar, P.K. Shishodia, R.M. Mehra, H. Okada, A. Wakahara, A. Yoshida, *J. Luminescen* **126**, 800–806 (2007)
14. B. Guo, Z.R. Qiu, K.S. Wong, *Appl. Phys. Lett.* **82**, 2290–2292 (2003)
15. M. Ferhat, A. Zaoui, R. Ahuja, *Appl. Phys. Lett.* **94**, 142502– 142504 (2009)
16. S. Suresh, *Appl. Nanosci.* **4**, 325–329 (2014)
17. S. Suresh, C. Arunseshan, *Appl. Nanosci.* **4**, 179–184 (2014)

18. Suresh Sagadevan, Isha Das, Jiban Podder, Journal of Materials Science: Materials in Electronics, 27(2016) 13016–13021
19. Devadoss Mangalam Durai Manoharadoss Prabakaran, Karuppasamy Sadaiyandi, Manickam Mahendran, Suresh Sagadevan, Materials Research, 19(2016) 478-482
20. Suresh Sagadevan, Isha Das, Preeti Singh, Jiban Podder, Journal of Materials Science: Materials in Electronics, 28, (2017) 1136–1141
21. Suresh Sagadevan, Isha Das Kaushik Pal, Priya Murugasen, Prithi Singh, J Mater Sci: Mater Electron DOI 10.1007/s10854-016-6180-z, (2016).